Signaling and Regulation

Molecular Cancer Research

Oxytocin Induces the Migration of Prostate Cancer Cells: Involvement of the Gi-Coupled Signaling Pathway

Miao Zhong, Maryam L. Boseman, Ana C. Millena, and Shafiq A. Khan

Abstract

Expression of genes that encode oxytocin (*OXT*) and vasopressin (*AVP*) and their cognate receptors in normal and diseased prostates are only partially characterized. Reverse transcription and PCR were used to examine the expression of these genes in normal prostate epithelial and stromal cell lines, k-ras–transformed prostate epithelial cell lines, and in four prostate cancer cell lines. Secreted and cell-associated OXT peptide was measured by an enzyme immunoassay. OXT and its receptor (OXTR) were expressed in all eight prostate cell lines. Cell-associated OXT peptide was also found in all prostate epithelial cell lines except in DU145 cells. Neither *AVP* nor its cognate receptors (V1a receptor and V2 receptor) were expressed in any prostate cell line examined. These data point to the OXTR as the primary target of *OXT* and *AVP*, and suggest that *OXT* might be an autocrine/paracrine regulator in human prostate. We found that *OXT* induces the migration of PC3 and PC3M, but not DU145 prostate cancer cells. The effect of *OXT* is distinct from the epidermal growth factor (EGF)–induced migration of prostate cancer cells, in which ERK1/2 and EGF receptor kinase activities were required. When cells were pretreated with pertussis toxin, the effect of *OXT*, but not EGF, on cell migration was abolished. Pretreatment with the cyclic AMP analogue, 8-Br-cAMP, did not affect *OXT*-induced cell migration, which eliminated the nonspecific effect of pertussis toxin. We conclude that a Gi-dependent mechanism is involved in OXTR-mediated migration of prostate cancer cells, and indicates a role for OXTR in prostate cancer metastasis. *Mol Cancer Res; 8(8); 1164–72. ©2010 AACR.*

Introduction

Oxytocin (*OXT*) and vasopressin (*AVP*) are highly homologous peptide hormones that have diverse physiologic functions (1). *OXT* regulates the contractility of uterine smooth muscle at parturition and mammalian myoepithelium during lactation. *AVP*, on the other hand, is associated with vasoconstriction, antidiuretic, and adrenocorticotropic hormone–releasing activities. The differences in the physiology of the two hormones results from the activation of a subset of G protein–coupled receptors (GPCR; refs. 2-7). To date, four GPCRs have been identified as targets of *OXT* and *AVP*. The AVP type 1a (*V1aR*), type 1b (*V1bR*), and OXT receptors (*OXTR*) activate the GTP-binding protein Gαq to stimulate phospholipase Cβ, whereas the AVP type 2 receptor (*V2R*) preferentially couples to Gαs to stimulate cyclic AMP (cAMP) accumulation. OXTR was also found to couple to Gi and Gh under specific conditions (8, 9). In turn, these G proteins may couple to distinct signaling pathways in different cell types.

OXT and *AVP* have been shown to function as autocrine/paracrine regulators of tumor progression in several types of cancers (10-13). *OXT* acts as a mitogenic factor to induce cell proliferation in Kaposi's sarcoma, but does not affect tumor cell migration *in vitro* or angiogenesis *in vivo* (12). *OXT* functions as a paracrine factor to induce proliferation and cell migration in human breast tumor–derived endothelial cells (14). On the other hand, it inhibits cell growth in breast cancer cell lines (10). *AVP* stimulates steroid secretion in adrenocortical tumors that express the endogenous *V1aR* (13). *OXT* and *AVP* are expressed in small cell lung carcinoma and exert mitogenic effects in these cell lines (11). The variable effects of OXT on cell growth are potentially attributed to the distribution of OXTR in different membrane microdomains and are a consequence of coupling to different signaling pathways (15).

OXT treatment has been shown to increase epithelial cell growth, 5α-reductase activity, and contractility in normal prostate (16-18). *OXT* and *AVP* have also been implicated in prostate cancer progression (19, 20). Although some clinical studies have shown that high levels of *AVP* peptide are present in metastatic prostate adenocarcinomas (19), the functional relevance of *AVP* and the identities of the components for *AVP* signaling in prostate cancer cells are not known. OXTR has been detected in normal stromal

Authors' Affiliation: Center for Cancer Research and Therapeutic Development, Clark Atlanta University, Atlanta, Georgia

Corresponding Author: Shafiq A. Khan, Center for Cancer Research and Therapeutic Development, Clark Atlanta University, 223 James P. Brawley Drive, SW, Atlanta, GA 30314. Phone: 404-880-6795; Fax: 404-880-6756. E-mail: skhan@cau.edu

doi: 10.1158/1541-7786.MCR-09-0329

©2010 American Association for Cancer Research.

and epithelial cell lines, as well as in DU145 prostate cancer cell line (20, 21). It has also been detected in tissues from hyperplastic and neoplastic prostates (20, 21). However, data on the expression of OXT in prostate cells are still controversial (20-22). Recently, atosiban, an OXTR antagonist that blocks the OXT-activated Gq pathway, was shown to inhibit cell proliferation by activating the Gi-mediated pathway in DU145 cells that express the endogenous OXTR (15). Hence, the influence of OXT on prostate cancer progression is dependent on the status of activated intracellular signaling pathways. Moreover, it also seems that ERK phosphorylation is a convergent point of both Gi- and Gq-mediated signal pathways (15). Currently, there is no definitive functional assay available that reflects the coupling of OXTR to the Gi-mediated signaling pathway. In the present study, we show the expression of OXT and OXTR in prostate cells and that OXT stimulates the migration of prostate cancer cells. In addition, we provide evidence which supports the involvement of the Gi-coupled signaling pathway in OXT-induced prostate cancer cell migration.

Materials and Methods

Chemicals

Human *OXT*, pertussis toxin, PD098059, 8-Br-cAMP, and bovine serum albumin were obtained from Sigma. AG1478 was obtained from Calbiochem. L-371,267 was obtained from Tocris. Rat tail collagen and transwell inserts were obtained from BD Biosciences. Superfine agarose was purchased from U.S. Biological. Cell culture reagents were obtained from Mediatech, Inc. Trizol and epidermal growth factor (EGF) were obtained from Invitrogen. Taq polymerase was purchased from Lucigen. Moloney murine leukemia virus reverse transcriptase and oligo-dT primer were purchased from Promega. All primers were purchased from IDT.

Cell culture and cell treatments

Normal prostate basal epithelial cells (PrEC), immortalized prostate luminal epithelial cell line (RWPE1), k-ras–transformed RWPE1 (RWPE2), normal prostate stromal cells (PrSC, non–smooth muscle type), and prostate cancer cell lines (LNCaP, DU145, and PC3) were obtained from American Type Culture Collection. LNCaP is an androgen-dependent cell line isolated from a lymph node lesion, whereas DU145 and PC3 are androgen-independent cell lines derived from brain and bone metastatic sites, respectively (23). PC3M, derived from a PC3 xenograft (24), was provided by Dr. Girsh Shah from the University of Louisiana (Monroe, LA). PrEC, RWPE1, and RWPE2 were maintained in Keratinocyte Growth Medium (Invitrogen). LNCaP cells were maintained in RPMI 1640 supplemented with 250 μg/mL of gentamycin and 10% fetal bovine serum. DU145, PC3, and PC3M cell lines were maintained in MEM supplemented with 5% fetal bovine serum.

Based on a report (25), four doses (0.1, 1, 10, and 100 nmol/L) were chosen to examine *OXT*-dependent cell migration. The 100 nmol/L dose of *OXT* was found to be an optimal concentration for cell migration, and was applied to subsequent mechanistic studies. The specific OXTR antagonist L-371,257 (1 μmol/L) was used to examine whether OXTR is the primary target of OXT (100 nmol/L) to mediate the migration of PC3M prostate cancer cells (25). To study the potential involvement of pertussis toxin–sensitive G proteins, cells were pretreated with 100 ng/mL of pertussis toxin overnight before experiments; no more pertussis toxin was required during the course of experiments. Cells were pretreated with various inhibitors for 30 minutes prior to treatment with agonists. Trypan blue exclusion assay did not detect any change in cell viability with different treatments.

Cell migration assay

In vitro cell migration assay was done using 24-well transwell inserts (8 μm; ref. 26). Briefly, cells were washed once with MEM and harvested from cell culture dishes by EDTA-trypsin into 50 mL conical tubes. The cells were centrifuged at 500 × *g* for 10 minutes at room temperature; the pellets were resuspended into MEM supplemented with 0.2% bovine serum albumin at a cell density of 3×10^5 cells/mL. The outside of the transwell insert membrane was coated with 50 μL of rat tail collagen (50 μg/mL) overnight at 4°C. The next day, aliquots of rat tail collagen (50 μL) were added into the transwell inserts to coat the inside of the membranes. The inserts were left to stand for 1.5 hours at room temperature before being washed thoroughly with 3 mL of MEM. Chemoattractant solutions were made by diluting OXT (0.1, 1, 10, and 100 nmol/L) or EGF (3 ng/mL) into MEM supplemented with 0.2% bovine serum albumin. MEM containing 0.2% bovine serum albumin served as a control medium. EGF was used as a positive control (27). Control and chemoattractant solutions (400 μL) were added into different wells of a 24-well plate. Aliquots of 100 μL cell suspension were loaded into transwell inserts that were subsequently placed into the 24-well plate. The transwell insert-loaded plate was placed in a cell culture incubator for 5 hours. At the end of the incubation, transwell inserts were removed from the plate individually; the cells inside transwell inserts were removed by cotton swabs. The cleaned inserts were fixed in 300 μL of 4% paraformaldehye (pH 7.5) for 20 minutes at room temperature. Cells on the outside of the transwell insert membrane were stained using HEMA 3 staining kit (Fisher Scientific, Inc.). The number of stained cells was counted in four nonoverlapping low-power fields of a light microscope, and the average number of cells reflected the cell migration status in each transwell insert. To avoid experimental bias, a systematic random sampling technique was applied in the selection of representative fields, in which sample preparation and handling was executed by different persons.

Results were expressed as migration index, which is defined as the average number of cells per field for test

substance / the average number of cells per field for the medium control. Each experiment was repeated at least three times using a different cell preparation.

Enzyme immunoassay of OXT peptide

Six prostate epithelial cell lines (RWPE1, RWPE2, LNCaP, DU145, PC3, and PC3M) were cultured in 100 mm dishes to 80% confluence. Fresh keratinocyte growth medium (without supplements) was added and cells were cultured for 24 hours. The supernatants were collected and centrifuged to remove cellular debris. Attached cells were lysed as described earlier (28). Two independent sets of samples were prepared for the detection of OXT peptide. Concentrations of OXT peptide were measured in the cell lysate and culture supernatant samples using an enzyme immunoassay kit (Assay Designs) according to the instructions provided by the manufacturer. The kit is able to detect OXT peptide levels greater than 11.7 pg/mL. Total protein concentrations were measured as described previously (28) and OXT concentrations were normalized with total protein concentrations. All samples were analyzed in the same assay and intra-assay variation was <10%.

RNA extraction, reverse transcription-PCR, and quantitative real-time PCR

Total RNAs were extracted from cells using Trizol and the RNA content was determined with UV spectraphotometer (Bio-Rad). First-strand cDNA was prepared from 2 μg of total RNA using 200 units of Moloney murine leukemia virus reverse transcriptase and 20 μmol/L of oligo-dT primer in 50 μL reaction buffer at 37°C for 1.5 hours. Reverse transcription (RT) reaction was stopped by heating samples at 65°C for 5 minutes. Control samples were also prepared in parallel by omitting reverse transcriptase. The cDNA sample from HeLa cells was used as a negative control for OXT and OXTR (29).

The cDNAs were amplified with PCR to detect the expression of *OXT, OXTR, AVP, V1aR, V2R*, and *L19* genes using specific primers listed in Table 1. A cDNA template (2.5 μL) was used for the detection of *OXT, OXTR, AVP, V1aR*, and *V2R*, whereas 0.5 μL of cDNA template was used for L19. The cDNA template was mixed with 0.4 μmol/L of primers, 0.5 mmol/L of deoxynucleotide triphosphate, and 1 unit of Taq in a final volume of 10 μL. PCR samples were denatured at 94°C for 2 minutes, followed by 30 to 35 cycles of the following process: denaturation at 94°C for 30 seconds, annealing at 60°C for 30 seconds, and extension at 72°C for 60 seconds. A final extension for 10 minutes was followed up after the cycles were completed.

Nested PCR was also used to amplify OXT cDNA to enhance the specificity and sensitivity. Reaction volumes for both external and internal PCR amplifications were 10 μL. A volume of 0.5 μL of cDNA template and 0.1 μmol/L of external primers were used for external PCR. A volume of 0.4 μL external PCR product was then used as the template for internal PCR along with 0.4 μmol/L of internal primers.

PCR products were separated by electrophoresis on a 3% agarose gel containing ethidium bromide. DNA bands were visualized under UV light and images were documented using the Bio-Rad gel imager.

For quantitative real-time PCR, cDNA samples (2 μL) were mixed with 0.2 μmol/L of primers and 2× SYBR Green supermix (Bio-Rad) in a final volume of 25 μL in a 96-well PCR plate and placed in an iCycler thermal cycler (Bio-Rad) for PCR with the following steps: 1, 95°C for 3 minutes; 2, 95°C for 15 seconds; 3, 60°C for 1 minute; 4, repeating steps 2 and 3 for 40 times; 5, 95°C for 1 minute; 6, 55°C for 1 minute; 7, 55°C for 10 seconds; 8, repeating step 7 for 100 times. Melting curves were examined for the quality of PCR amplification of each sample. Calculations were done using the ΔΔCt method (30), in which the expression of OXTR in PrEC was first normalized

Table 1. Primers for RT-PCR and quantitative PCR of *OXT, AVP*, and their receptors

Genes	Gene ID	Primers	Sequences (5′-3′)	Location	Product size (bp)
AVP	189095260	AVP-F	GGGGTCCACCTGTGTGC	28-44	151
		AVP-R	GGGAGGCACTGTCTCAGC	178-161	
OXT	12707574	OXT-1F	GCGGTCTTGGGCCTCTGC	331-349	100
		OXT-1R	TCGGAGCCATCAAGTTTCAGC	430-410	
		OXT-2F	GGAGGAGAACTACCTGCCGT	264-283	218
		OXT-2R	ACCATTTCTGGGGTGGCTAT	481-462	
OXTR	32307151	OXTR-F	GCAGGGCATCCCAACTCG	275-292	189
		OXTR-R	AAATGAGCGGGAATCCTCTACC	463-442	
V1aR	33149325	V1aR-2F	CGGGCGGCATCTTTGTGG	2636-2653	340
		V1aR-R	GCAGTGATGGTGATGGTAGGG	2975-2955	
V2R	225903383	V2R-F	CCATTGAACTTGCTCCTCAGG	1-13	227
		V2R-R	GCCACAGCCACAAAGACTATG	226-206	
L19	68216257	L19-F	GAAATCGCCAATGCCAACTC	306-325	406
		L19-R	TCTTAGACCTGCGAGCCTCA	711-692	

to the expression of L19 and then expressed relative to the corresponding value in other cell lines.

Statistical analysis

Data from multiple independent experiments are expressed as mean ± SEM. ANOVA and Duncan's modified multiple range test were used to examine significance between multiple treatments.

Results

Expression of OXT and *AVP* and their cognate receptors in prostate cell lines

To investigate the potential functions of OXT and *AVP* in prostate cancer progression, steady state mRNA levels of OXT and *AVP* and their cognate receptors were determined by RT-PCR in several human prostate cell lines. As shown in Fig. 1, OXTR mRNA was present in all cell lines examined (PrSC, PrEC, RWPE1, RWPE2, LNCaP, DU145, PC3, and PC3M). It seemed that OXTR mRNA levels were lower in normal epithelial cell lines (PrEC, RWPE1, and RWPE2) but relatively high in prostate cancer cells, especially in PC3 and PC3M cells. Quantitative real-time PCR was used to determine the relative expression of OXTR in prostate epithelial cell lines. These data confirmed higher expression of OXTR mRNA in advanced prostate cancer cell lines (Fig. 1B).

OXT was detected with PCR from cDNA samples derived from RNA extractions of PrEC, PrSC, and DU145; DNA sequencing verified that the resulting PCR amplicon contained the amplified portion of OXT gene (data not shown). A nested PCR strategy was subsequently applied to enhance the detection specificity and sensitivity. As shown in Fig. 1A, OXT mRNA was present in PrEC, RWPE1, RWPE2, LNCaP, DU145, PC3, and PC3M cells. In contrast, neither *AVP* nor its cognate receptor mRNAs (*V1aR* and *V2R*) were detectable in any of the cell lines used in this study (data not shown). In addition, neither OXT nor OXTR mRNA was detected in the RNA samples processed without reverse transcription (no RT controls) and in the cDNA samples from HeLa cells which have been shown previously to not express OXTR (ref. 29; Fig. 1).

To examine whether OXT gene is translated in these prostate cell lines, the cell lysates and conditioned culture supernatants were collected from RWPE1, RWPE2, LNCaP, DU145, PC3, and PC3M prostate cell lines. The OXT peptide was found in cell lysates from all cell lines except DU145 cells. The levels of OXT peptide ($n = 2$) in RWPE1, RWPE2, LNCaP, PC3, and PC3M were 47.4 (54.0/40.7), 16.0 (19.0/13.0), 3.1 (3.5/2.7), 13.5 (3.0/24.0), and 129.2 (148.6/109.8) pg/mg protein, respectively. However, the OXT peptide was not detectable in the culture supernatants, presumably due to the sensitivity of the enzyme immunoassay.

Differential influences of OXT on migration of prostate cancer cells

OXT was shown to induce the migration of human endothelial cells that originated from different tissues (14, 31). In the present study, we found for the first time that OXT treatment stimulated cell migration in PC3 and PC3M cell lines but not in the DU145 cell line (Fig. 2A). On the other hand, EGF (3 ng/mL) induced cell migration in all three cell lines (Fig. 2A). As shown in Fig. 2A, the basal motility was relatively higher in PC3 and PC3M cells when compared with DU145 cells under the same experimental conditions. EGF treatment significantly increased migration in PC3 cells (2.7 ± 0.16-fold) as well as in PC3M cells (1.8 ± 0.18-fold). OXT also induced a dose-dependent increase in the migration of PC3 and PC3M cells, and the effects of OXT on migration were comparable between these two cell lines (Fig. 2B). A significant increase in cell migration was observed when PC3 and PC3M were treated with OXT at the low dose

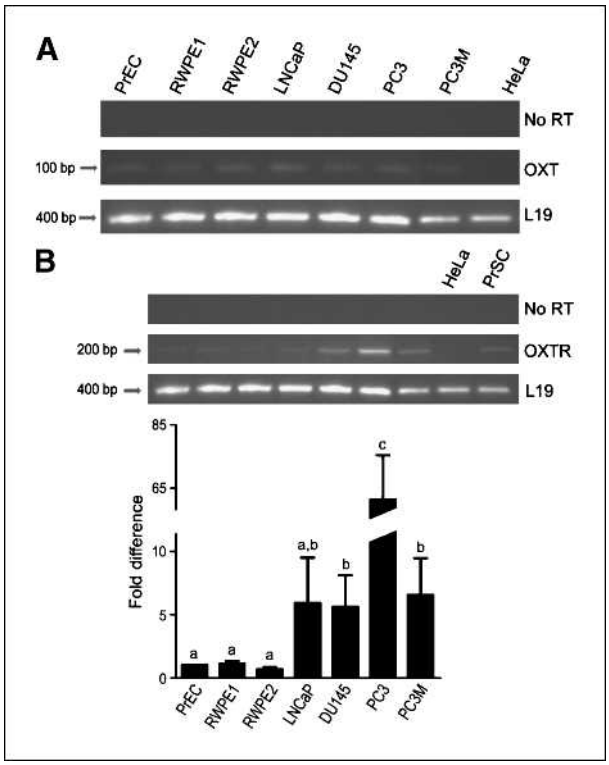

FIGURE 1. Expression of OXT and its cognate receptor mRNA in human prostate cell lines. To distinguish from potential genomic DNA contamination, mRNA regions that span an intron were chosen for amplification of OXT, OXTR, and L19. A, OXT mRNA was detected by nested PCR in PrEC, RWPE1, RWPE2, LNCaP, DU145, PC3, and PC3M. The HeLa cDNA sample was included as a negative control. A panel of no RT samples derived from the same RNAs is also included. Thirty cycles were applied in both external and internal amplifications. Similar results were replicated in at least three independent experiments. B, real-time PCR to quantitate the relative expression of OXTR in the cell lines described above. L19 was used as a template control. Columns, mean analyzed by ANOVA and Duncan's modified range test; bars, SEM ($n = 3$). Significant differences between groups in a given category ($P < 0.05$) are designated with different lowercase letters. The expression of OXTR in PrEC is set as the standard for comparison. Top, PCR amplification of OXTR and L19 in a PrSC sample and in a representative set of samples used in the quantitative PCR. A panel of no RT controls is also shown. The HeLa cDNA sample was also included as a negative control. OXTR was amplified with 35 cycles and L19 with 30 cycles.

of 1 nmol/L (32). As shown in Fig. 3, the effect of OXT (100 nmol/L) was completely inhibited by the pretreatment of PC3M cells with a specific OXTR antagonist (L-371,267; 1 μmol/L).

Distinct molecular mechanisms underlying the migration of prostate cancer cells induced by activated OXTR versus EGF receptor

Activated ERK1/2 and EGF receptor (EGFR) have been shown to phosphorylate multiple cytoskeleton proteins and to promote cell migration (33, 34). To find out potential involvements of EGFR and ERK1/2 in OXT-induced cell migration, PC3M cells were treated with either an EGFR kinase inhibitor (AG1478; 1 μmol/L) or an MEK inhibitor (PD098059; 20 μmol/L) to prevent ERK1/2 activation. As shown in Fig. 4A, OXT (100 nmol/L) induced an approximately 2-fold increase in the migration of PC3M cells; neither of the inhibitors was able to completely inhibit the OXT-induced migration. EGF (3 ng/mL) induced a 1.9-fold increase in migration of PC3M cells. Pretreatments with AG1478 and PD098059 completely blocked EGF-stimulated cell migration (Fig. 4B).

Gi-coupled pathway mediates the OXTR-induced migration of prostate cancer cells

Because OXTR has been shown to couple to multiple G proteins, including Gq and Gi, the involvement of Gi in OXT-induced cell migration was examined by treating cells overnight with pertussis toxin (100 ng/mL). As shown in Fig. 5, pertussis toxin alone did not affect the basal motility of PC3M cells. However, it completely blocked the effects of OXT on cell migration. Previous studies have reported on the ability of pertussis toxin to inhibit Gq-dependent pathways operating downstream of the activated OXTR (35-37). This inhibitory action is mediated via activated protein kinase A (PKA) rather than being a direct consequence of the inhibition of Gi proteins. To examine the potential influence of PKA activity on OXT-induced cell

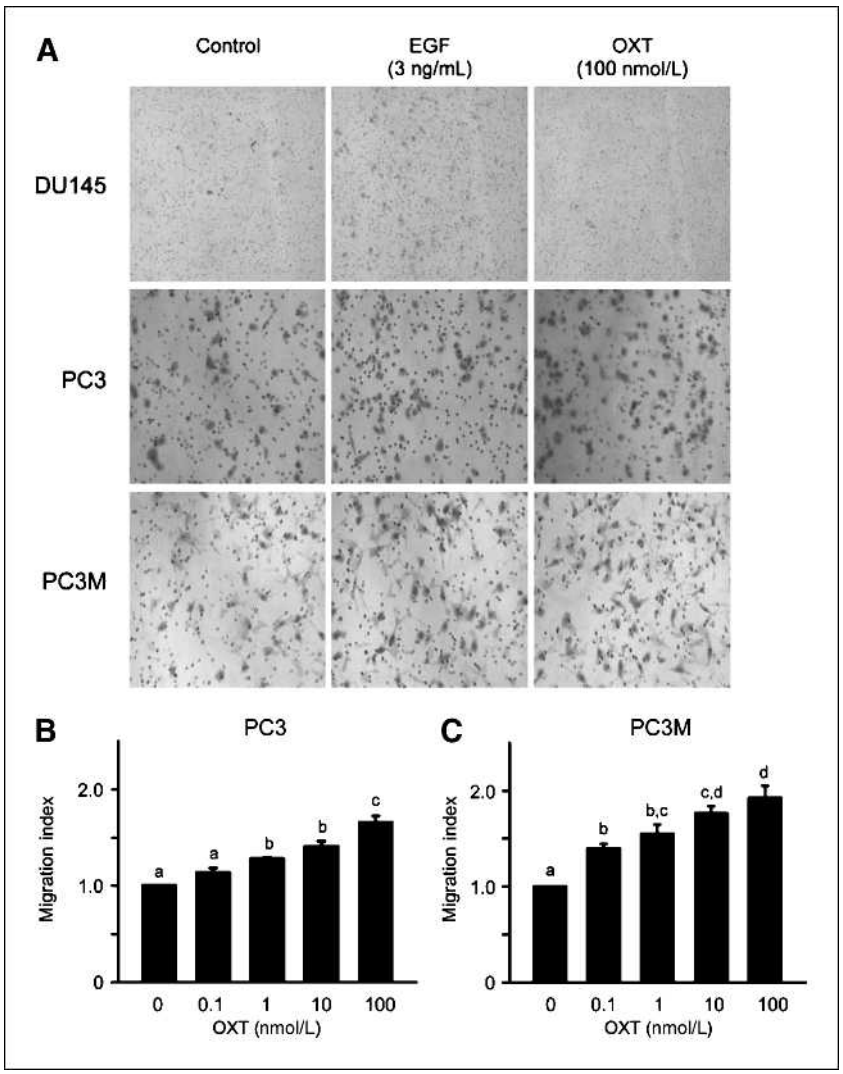

FIGURE 2. Differential effects of OXT on migration of prostate cancer cell lines. A, representative images from different treatments of three prostate cancer cell lines (DU145, PC3, and PC3M). Original magnification, ×10. EGF (3 ng/mL) induced migration in all three cell lines. OXT (100 nmol/L) did not induce migration in DU145 cells. OXT dose-dependently induced migration in PC3 (B) and PC3M (C) cells in a transwell migration assay. Columns, mean; bars, SEM (B: $n = 4$; C: $n = 3$). Significant differences between treatments are designated by different lower case letters.

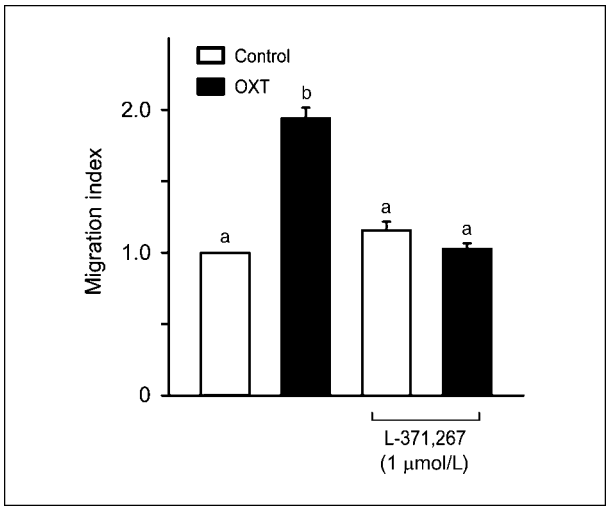

FIGURE 3. Blockage of OXT-induced cell migration by a specific OXTR antagonist (L-371,267). Pretreatment with L-371,267 (1 μmol/L) for 30 min completely blocked the migration of PC3M cells induced by OXT (100 nmol/L). Columns, mean; bars, SEM (n = 5). Significant differences between treatments are designated by different lower case letters.

migration, PC3M cells were pretreated for 30 minutes with 8-Br-cAMP (0.3 mmol/L), the cell-permeable cAMP analogue that activates PKA. The 8-Br-cAMP pretreatment did not exert any effect on OXT-induced cell migration, which excluded the involvement of PKA in the inhibitory effect of pertussis toxin. Similar effects of pertussis toxin and 8-Br-cAMP were also observed in PC3 cells (data not shown). The possibility of nonspecific effects of pertussis toxin was ruled out by the fact that it did not block EGF-induced cell migration (Fig. 5).

Discussion

The expression of genes that encode OXT, *AVP*, and their cognate receptors in normal and diseased prostates and their biological effects are only partially understood. In the present study, mRNAs of OXT and OXTR were found to be expressed in eight human prostate cell lines. On the other hand, mRNAs of *AVP* and AVP receptors (*V1aR* and *V2R*) were not detected.

The expression of OXT has been extensively investigated in prostate tissues and cells with controversial results (20, 22, 38). Using a nested PCR strategy in the present study, OXT mRNA was found to be present in all prostate cell lines examined (PrSC, PrEC, RWPE1, RWPE2, LNCaP, DU145, PC3, and PC3M). In addition, cell-associated OXT peptide was also detected in several prostate cells. These data, together with previous studies (21, 22), support the expression of OXT mRNA and peptide in human prostate tissues and cells, suggesting a potential autocrine/paracrine role of OXT in functions of human prostate in normal and disease states. *AVP* and its cognate receptors have been implicated in tumor progression in several types of cancers (11, 13). However, there has been very limited information about their roles in prostate cancer. AVP and AVP receptor mRNAs were not detected by PCR in any of the prostate cell lines examined in the present study. This finding contrasts with observations of some clinical studies, in which high levels of AVP peptide were shown to be present in metastatic prostate adenocarcinomas (19). The absence of AVP receptor expression in the prostate is supported by microarray analysis information from the Gene Expression Omnibus profile database on the National Center for Biotechnology Information web site. These findings exclude their potential importance in prostate functions. Previously, AVP treatment had been reported to increase prostatic muscle tone and induce prostate contraction (17), which might be mediated by the activated OXTR. OXTR mRNAs have previously been detected in specific cell types in prostate tissues of several species (18, 20, 22). The expression of OXTR mRNA in PrSC (present study) supports its reported function to induce prostate gland contraction (17, 21). An increased expression of OXTR was found in prostate neoplastic

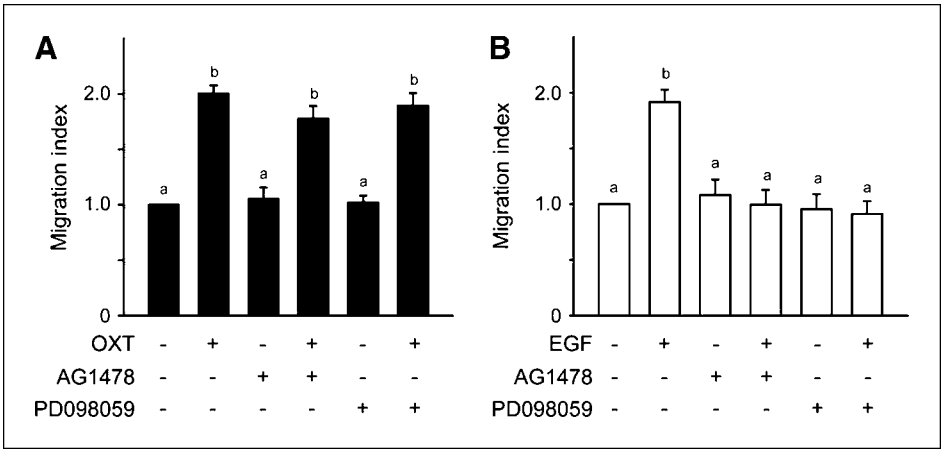

FIGURE 4. Potential contributions of EGFR and ERK1/2 activities to the migration of prostate cancer cells. Pretreatments with PD098059 (20 μmol/L) and AG1478 (1 μmol/L) did not influence the OXT (100 nmol/L) induced migration of PC3M cells (A), but completely blocked the EGF (3 ng/mL) induced migration of PC3M cells (B). Columns, mean; bars, SEM (n = 4). Significant differences between treatments are designated by different lower case letters.

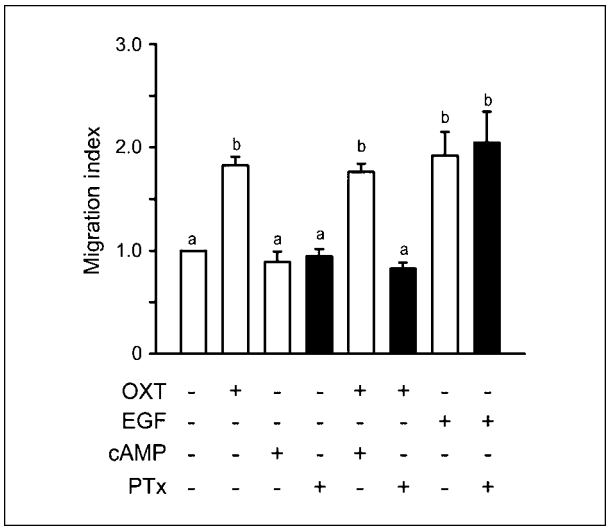

FIGURE 5. Effects of pertussis toxin and cAMP on OXT and EGF effects on migration of prostate cancer cells. Overnight treatment with pertussis toxin (100 ng/mL) completely inhibited the OXT (100 nmol/L) induced migration of PC3M cells, but did not block the EGF (3 ng/mL) induced cell migration. Pretreatment with 8-Br-cAMP (0.3 mmol/L) did not influence the effect of OXT. Columns, mean; bars, SEM (n = 4). Significant differences between treatments are designated by different lower case letters.

epithelial cells when compared with hyperplastic cells (20). Consistent with this observation, our quantitative PCR data shows that expression of OXTR is comparable in three normal epithelial cells but at higher levels in all prostate cancer cell lines. Hence, increased expression of OXTR may be a general phenomenon in prostate carcinomas.

OXTR couples to multiple G proteins including Gq and Gi. In turn, these G proteins may convey OXT signaling to different intracellular pathways leading to distinct cellular functions (15). Chemotaxis has been associated with the activation of GPCRs that couple exclusively to Gi (39, 40). Hence, OXT would induce the migration of prostate cancer cells if endogenous OXTRs couple effectively to the Gi-dependent pathway.

OXT treatment was found to induce cell migration in PC3 and PC3M but not in DU145 cell lines, whereas EGF treatment induced cell migration in all three cell lines. Pretreatment with a specific OXTR antagonist (L-371,267) completely blocked OXT-induced migration in PC3M cells, suggesting the involvement of activated OXTR. A clear difference was observed in the migration of DU145 cells in response to OXT and EGF, which suggests that multiple signaling mechanisms are possibly used by different hormones and growth factors to promote cell migration in prostate cancer. Transactivation of EGFR is a common consequence following the activation of many GPCRs that couple to diverse types of G proteins, and also serves as a convergent point for activated GPCRs to promote migration and invasion in kidney and bladder cancer cell lines (34). There are several lines of evidence that support cell migration independent of Gi activation in different types of cells (41). Hence, it is tempting to speculate that transactivation of EGFR may function as a general mechanism to converge signal inputs from different types of activated G proteins to influence cell migration. Activated OXTR stimulates ERK1/2 phosphorylation by transactivating EGFR through Gβγ liberated from Gq heterotrimeric complexes in different cell lines (35). However, it has recently been shown that transactivation of EGFR is not involved in OXTR-induced migration in human umbilical vein endothelial cells, despite the fact that the OXTR-mediated Gαq-phospholipase C pathway is involved (31). In the present study, we observed the differential effects of OXT and EGF on migration of DU145 cells. This data is not consistent with the potential involvement of EGFR in OXTR signaling that leads to cell migration. As additional evidence, OXT stimulated a substantial migration of PC3M cells in the presence of EGFR kinase inhibitor (AG1478) or MEK inhibitor (PD098059) which blocks ERK1/2 activation. Activated ERK1/2 have been shown to interact with and phosphorylate multiple cytoskeletal proteins (33). ERK1/2 activities are also required for EGFR-mediated migration in several types of cells (42, 43). In line with these findings, the EGF-induced migration of PC3M cells was effectively blocked by pretreatments with PD098059 and AG1478. Our data suggest that ERK1/2-dependent cell migration does not contribute to the migratory process induced by activated OXTR in prostate cancer cells.

Although activated OXTR relies on a Gαq-phospholipase C–dependent pathway to induce migration of human umbilical vein endothelial cells (31), it mediates the migration of PC3 and PC3M cells predominantly through the Gi-dependent pathway because the effect of OXT was abolished by pertussis toxin pretreatment. Pertussis toxin ADP-ribosylates and inhibits Gαi activation. On the other hand, it might influence cell functions through intracellular signaling events other than Gi inhibition (44), such as PKA activation to perturb OXTR signaling through Gq-dependent pathways (35-37). Pretreatment with the cAMP analogue, 8-Br-cAMP, did not affect OXT-induced migration of PC3 and PC3M cells. This data suggests that PKA activation is not involved in the inhibitory effects of pertussis toxin, and in turn, strongly supports the role of Gi proteins in OXT-induced migration in prostate cancer cells. In addition, pertussis toxin pretreatment did not inhibit the EGF-induced migration of PC3M cells. This data excludes any nonspecific influence of pertussis toxin on the cell migration process.

In summary, we provide evidence that supports the expression of OXT and OXTR in several types of prostate cell lines, which is consistent with a potential autocrine/paracrine function of OXT in normal and diseased prostates. The lack of AVP and its receptors suggests that OXTR is the primary target of OXT and *AVP* in the prostate. Finally, OXT treatment induces the migration of PC3 and PC3M cells, which is mediated by the Gi-coupled pathway. Our data suggest that activation of OXTR might contribute to prostate cancer invasion and metastasis.

Disclosure of Potential Conflicts of Interest

No potential conflicts of interest were disclosed.

Acknowledgments

We are grateful to Dr. Natalya Klueva and Paulette Dillard for their help in this study.

Grant Support

NIH (RCMI 5G12RR003062 and NCMHD 1P20MD002285-01) and Georgia Research Alliance.

The costs of publication of this article were defrayed in part by the payment of page charges. This article must therefore be hereby marked *advertisement* in accordance with 18 U.S.C. Section 1734 solely to indicate this fact.

Received 07/24/2009; revised 06/15/2010; accepted 06/16/2010; published OnlineFirst 07/27/2010.

References

1. Gimpl G, Fahrenholz F. The oxytocin receptor system: structure, function, and regulation. Physiol Rev 2001;81:629–83.
2. Sugimoto T, Saito M, Mochizuki S, Watanabe Y, Hashimoto S, Kawashima H. Molecular cloning and functional expression of a cDNA encoding the human V1b vasopressin receptor. J Biol Chem 1994;269:27088–92.
3. Morel A, O'Carroll AM, Brownstein MJ, Lolait SJ. Molecular cloning and expression of a rat V1a arginine vasopressin receptor. Nature 1992;356:523–6.
4. Lolait SJ, O'Carroll AM, McBride OW, Konig M, Morel A, Brownstein MJ. Cloning and characterization of a vasopressin V2 receptor and possible link to nephrogenic diabetes insipidus. Nature 1992;357:336–9.
5. Kimura T, Tanizawa O, Mori K, Brownstein MJ, Okayama H. Structure and expression of a human oxytocin receptor. Nature 1992;356:526–9.
6. de Keyzer Y, Auzan C, Lenne F, et al. Cloning and characterization of the human V3 pituitary vasopressin receptor. FEBS Lett 1994;356:215–20.
7. Birnbaumer M, Seibold A, Gilbert S, et al. Molecular cloning of the receptor for human antidiuretic hormone. Nature 1992;357:333–5.
8. Strakova Z, Soloff MS. Coupling of oxytocin receptor to G proteins in rat myometrium during labor: Gi receptor interaction. Am J Physiol 1997;272:E870–6.
9. Baek KJ, Kwon NS, Lee HS, Kim MS, Muralidhar P, Im MJ. Oxytocin receptor couples to the 80 kDa Gh α family protein in human myometrium. Biochem J 1996;315:739–44.
10. Sapino A, Cassoni P, Stella A, Bussolati G. Oxytocin receptor within the breast: biological function and distribution. Anticancer Res 1998;18:2181–6.
11. Pequeux C, Keegan BP, Hagelstein MT, Geenen V, Legros JJ, North WG. Oxytocin- and vasopressin-induced growth of human small-cell lung cancer is mediated by the mitogen-activated protein kinase pathway. Endocr Relat Cancer 2004;11:871–85.
12. Cassoni P, Sapino A, Deaglio S, et al. Oxytocin is a growth factor for Kaposi's sarcoma cells: evidence of endocrine-immunological cross-talk. Cancer Res 2002;62:2406–13.
13. Arnaldi G, Gasc JM, de Keyzer Y, et al. Variable expression of the V1 vasopressin receptor modulates the phenotypic response of steroid-secreting adrenocortical tumors. J Clin Endocrinol Metab 1998;83:2029–35.
14. Cassoni P, Marrocco T, Bussolati B, et al. Oxytocin induces proliferation and migration in immortalized human dermal microvascular endothelial cells and human breast tumor-derived endothelial cells. Mol Cancer Res 2006;4:351–9.
15. Reversi A, Rimoldi V, Marrocco T, et al. The oxytocin receptor antagonist atosiban inhibits cell growth via a "biased agonist" mechanism. J Biol Chem 2005;280:16311–8.
16. Plecas B, Popovic A, Jovovic D, Hristic M. Mitotic activity and cell deletion in ventral prostate epithelium of intact and castrated oxytocin-treated rats. J Endocrinol Invest 1992;15:249–53.
17. Bodanszky M, Sharaf H, Roy JB, Said SI. Contractile activity of vasotocin, oxytocin, and vasopressin on mammalian prostate. Eur J Pharmacol 1992;216:311–3.
18. Assinder SJ, Johnson C, King K, Nicholson HD. Regulation of 5α-reductase isoforms by oxytocin in the rat ventral prostate. Endocrinology 2004;145:5767–73.
19. Yamazaki T, Suzuki H, Tobe T, et al. Prostate adenocarcinoma producing syndrome of inappropriate secretion of antidiuretic hormone. Int J Urol 2001;8:513–6.
20. Cassoni P, Marrocco T, Sapino A, Allia E, Bussolati G. Evidence of oxytocin/oxytocin receptor interplay in human prostate gland and carcinomas. Int J Oncol 2004;25:899–904.
21. Whittington K, Assinder S, Gould M, Nicholson H. Oxytocin, oxytocin-associated neurophysin and the oxytocin receptor in the human prostate. Cell Tissue Res 2004;318:375–82.
22. Einspanier A, Ivell R. Oxytocin and oxytocin receptor expression in reproductive tissues of the male marmoset monkey. Biol Reprod 1997;56:416–22.
23. Sobel RE, Sadar MD. Cell lines used in prostate cancer research: a compendium of old and new lines—part 1. J Urol 2005;173:342–59.
24. Kozlowski JM, Fidler IJ, Campbell D, Xu ZL, Kaighn ME, Hart IR. Metastatic behavior of human tumor cell lines grown in the nude mouse. Cancer Res 1984;44:3522–9.
25. Tahara A, Tsukada J, Tomura Y, et al. Pharmacologic characterization of the oxytocin receptor in human uterine smooth muscle cells. Br J Pharmacol 2000;129:131–9.
26. Zigmond SH, Foxman EF, Segall JE. Chemotaxis assays for eukaryotic cells. Curr Protoc Cell Biol 2001;Chapter 12:Unit 12 1.
27. Kharait S, Dhir R, Lauffenburger D, Wells A. Protein kinase Cδ signaling downstream of the EGF receptor mediates migration and invasiveness of prostate cancer cells. Biochem Biophys Res Commun 2006;343:848–56.
28. Millena AC, Reddy SC, Bowling GH, Khan SA. Autocrine regulation of steroidogenic function of Leydig cells by transforming growth factor-α. Mol Cell Endocrinol 2004;224:29–39.
29. Kimura T, Makino Y, Bathgate R, et al. The role of N-terminal glycosylation in the human oxytocin receptor. Mol Hum Reprod 1997;3:957–63.
30. Pfaffl MW. A new mathematical model for relative quantification in real-time RT-PCR. Nucleic Acids Res 2001;29:e45.
31. Cattaneo MG, Chini B, Vicentini LM. Oxytocin stimulates migration and invasion in human endothelial cells. Br J Pharmacol 2008;153:728–36.
32. Whittington K, Connors B, King K, Assinder S, Hogarth K, Nicholson H. The effect of oxytocin on cell proliferation in the human prostate is modulated by gonadal steroids: implications for benign prostatic hyperplasia and carcinoma of the prostate. Prostate 2007;67:1132–42.
33. Yin G, Zheng Q, Yan C, Berk BC. GIT1 is a scaffold for ERK1/2 activation in focal adhesions. J Biol Chem 2005;280:27705–12.
34. Schafer B, Gschwind A, Ullrich A. Multiple G-protein-coupled receptor signals converge on the epidermal growth factor receptor to promote migration and invasion. Oncogene 2004;23:991–9.
35. Zhong M, Yang M, Sanborn BM. Extracellular signal-regulated kinase 1/2 activation by myometrial oxytocin receptor involves Gα(q)Gβγ and epidermal growth factor receptor tyrosine kinase activation. Endocrinology 2003;144:2947–56.
36. Singh SP, Anwer K, Wen Y, Sanborn BM. Inhibition of oxytocin-stimulated phosphoinositide turnover in rat myometrium by pertussis and cholera toxins may involve protein kinase A activation. Cell Signal 1992;4:619–25.

37. Dodge KL, Sanborn BM. Evidence for inhibition by protein kinase A of receptor/Gα(q)/phospholipase C (PLC) coupling by a mechanism not involving PLCβ2. Endocrinology 1998;139:2265–71.
38. Thackare H, Nicholson HD, Whittington K. Oxytocin—its role in male reproduction and new potential therapeutic uses. Hum Reprod Update 2006;12:437–48.
39. Neptune ER, Bourne HR. Receptors induce chemotaxis by releasing the βγ subunit of Gi, not by activating Gq or Gs. Proc Natl Acad Sci U S A 1997;94:14489–94.
40. Arai H, Tsou CL, Charo IF. Chemotaxis in a lymphocyte cell line transfected with C-C chemokine receptor 2B: evidence that directed migration is mediated by βγ dimers released by activation of Gαi-coupled receptors. Proc Natl Acad Sci U S A 1997;94:14495–9.
41. Juneja J, Casey PJ. Role of G12 proteins in oncogenesis and metastasis. Br J Pharmacol 2009;158:32–40.
42. Joslin EJ, Opresko LK, Wells A, Wiley HS, Lauffenburger DA. EGF-receptor-mediated mammary epithelial cell migration is driven by sustained ERK signaling from autocrine stimulation. J Cell Sci 2007;120:3688–99.
43. Glading A, Uberall F, Keyse SM, Lauffenburger DA, Wells A. Membrane proximal ERK signaling is required for M-calpain activation downstream of epidermal growth factor receptor signaling. J Biol Chem 2001;276:23341–8.
44. Schneider OD, Weiss AA, Miller WE. Pertussis toxin signals through the TCR to initiate cross-desensitization of the chemokine receptor CXCR4. J Immunol 2009;182:5730–9.